Enhanced Bearing Fault Diagnosis Based on Short-Time Zero Crossing Rate and Self-Organizing Maps with Feature Selection

HAROUN Smail#1, KOUBA Nour El Yakine*2

Laboratory of Electrical and Industrial Systems (LSEI),
Department of Electrical Engineering, Akli Mohand Oulhadj University - Bouira, Algeria
[1]s.haroun@univ-bouira.dz

* Laboratory of Electrical and Industrial Systems, University of Sciences and Technology Houari Boumediene, Algiers, Algeria
[2] nourelyakin.kouba@usthb.edu.dz

***Abstract*— This paper presents an enhanced methodology for detecting and classifying bearing faults in rotating electrical machines using a combination of Short-Time Zero Crossing Rate (STZCR) and Self-Organizing Maps (SOM). STZCR is applied to vibration signals to capture transient variations indicative of bearing defects. From this signal, multiple time-domain, frequency-domain, and fault-related frequencies are extracted. To optimize classification performance and reduce data dimensionality, two feature selection techniques—ReliefF and Genetic Algorithms—are implemented. The selected features are then classified using a SOM neural network, which effectively maps high-dimensional data into topological clusters representing different fault types. Experimental validation is performed using a standard bearing dataset under variable load conditions. The results show that frequency-domain features derived from STZCR provide more relevant information for classification, and that combining feature selection with SOM enhances the accuracy and efficiency of the diagnosis process. Furthermore, the use of feature selection—particularly the ReliefF method—significantly improves classification accuracy and overall diagnostic performance. The proposed approach demonstrates robustness and suitability for real-time bearing fault monitoring. Future work will focus on real-time implementation and fault severity analysis.**

***Keywords*— Bearing Fault Detection and Diagnosis; Short-Time Zero Crossing Rate (STZCR); Feature Selection; Self-Organizing Map (SOM); Vibration Analysis**

I. Introduction

Electrical rotating machinery is very common in wide range of industrial applications, playing a critical role in industries such as petrochemicals, power generation, and manufacturing. Key components like turbine-compressors in petrochemical plants or reactor coolant pumps in nuclear power plants rely on these machines for continuous, high-performance operation. Failure to detect early-stage faults in these systems can result in severe financial losses due to production downtime and, in some cases, even pose risks to human safety.

Bearing failures are one of the leading causes of breakdowns in rotating machines, accounting for approximately 41% of all machine failures [1]. Therefore, early detection of bearing defects is essential to prevent catastrophic failures and enhance system reliability. Various techniques for bearing fault detection and diagnosis (FDD) have been proposed in the literature, with vibration analysis being the most widely used and recognized method [2].

Vibration analysis covers numerous signal processing techniques [3,4], such as time-domain analysis, which monitors the variation of statistical parameters [5]. Frequency-domain analysis is also commonly employed, with the Fast Fourier Transform (FFT) being used to identify fault-related frequency components in the vibration spectrum [6]. However, these techniques are often inadequate for analyzing non-stationary signals, which are typically associated with machinery defects. Consequently, time-frequency domain techniques have been developed, including the Short-Time Fourier Transform (STFT) [7], the S-transform [8], Empirical Mode Decomposition (EMD) [9], Discrete Wavelet Transform (DWT), Continuous Wavelet Transform (CWT), and Wavelet Packet Transform (WPT) [10].

Rather than directly extracting features from the raw vibration signal, several transformation methods are applied to pre-process the data, improving fault detection and making the feature extraction process more efficient by reducing the complexity of the data. For instance, envelope analysis [11] demodulates high-frequency components

ISSN: 1737-9288

to uncover fault-related low-frequency modulations, making it easier to detect localized defects in bearings. Another method, the Short-Time Zero Crossing Rate (STZCR) technique particularly effective for detecting rapid changes in non-stationary signals [12]. STZCR measures the rate at which a signal crosses the zero axis within a short time window, capturing transient variations in the signal caused by faults. Its simplicity, combined with its ability to detect sudden variations without the need for prior knowledge of specific fault frequencies, makes it highly advantageous for real-time applications. Moreover, STZCR reduces the amount of data needed for fault classification, as it focuses on key transitions in the signal, leading to a faster and more efficient fault detection process.

Accurate fault detection and severity assessment require an automatic decision-making process to classify extracted features into different health condition categories [13]. To achieve this, several AI-based classification methods have been widely explored. These include traditional methods like Support Vector Machines (SVM) [14], and fuzzy logic systems [15]. In addition, various artificial neural networks have been applied, such as Multi-Layer Perceptron (MLP) [5], Radial Basis Function (RBF) networks [16], and Convolutional Neural Networks (CNNs) [17]. Self-Organizing Maps (SOM), an unsupervised neural network, have also been employed for clustering and fault classification [13,18]. These techniques have gained attention for their ability to improve overall accuracy and robustness in fault detection systems.

Fault detection based on AI-techniques can be hindered by noise and false alarms. Combining multiple feature extraction methods improves detection accuracy by capturing diverse fault signatures, but this also increases computational complexity [19]. To counter this, feature selection filters out the most relevant information, enhancing classifier accuracy while reducing processing time, making the system more efficient and suitable for real-time applications.

This paper introduces an innovative technique for bearing fault detection that integrates the Short-Time Zero Crossing Rate (STZCR) as a feature extraction method with a Self-Organizing Map (SOM) neural network for classification. To optimize the performance of the SOM classifier, feature selection techniques such as ReliefF and Genetic Algorithms are employed, ensuring the most relevant features are utilized for improved accuracy and effectiveness.

The structure of the paper is as follows: Section II outlines the framework of the proposed automatic bearing fault detection system. Section III details the experimental setup and presents the results obtained. Finally, Section IV concludes the paper and discusses directions for future work.

II. PROPOSED FAULT DIAGNOSIS SYSTEM

The proposed fault diagnosis system shown in Fig. 1 is centred around the analysis of vibration signals. These signals are collected using accelerometers from test motors operating under various bearing conditions. The methodology consists of three key stages: feature extraction, feature selection, and classification.

- *Feature Extraction:*

The Short-Time Zero Crossing Rate (STZCR) is derived from the vibration signal, providing a basis for extracting relevant features in both the time and frequency domains.

- *Feature Selection:*

To enhance the diagnostic process and reduce the dataset size, two feature selection methods are applied: ReliefF and Genetic Algorithms (GA). These techniques help identify and retain the most informative features for accurate classification.

- *Classification:*

The final stage of the process involves the use of a Self-Organizing Map (SOM) neural network, which serves as the classifier for the extracted and selected features.

A. Short Time Zero-crossing Rate

The zero-crossing rate (ZCR) measures how often the amplitude of a signal waveform crosses the zero line, either from positive to negative or vice versa [12]. This rate provides an indication of the frequency content of the signal, making it a useful tool in estimating its fundamental frequency [20].

ISSN: 1737-9288

Since the number of zero crossings per second is twice the signal's frequency, ZCR indirectly conveys valuable frequency information that can be very relevant for bearing faults diagnosis.

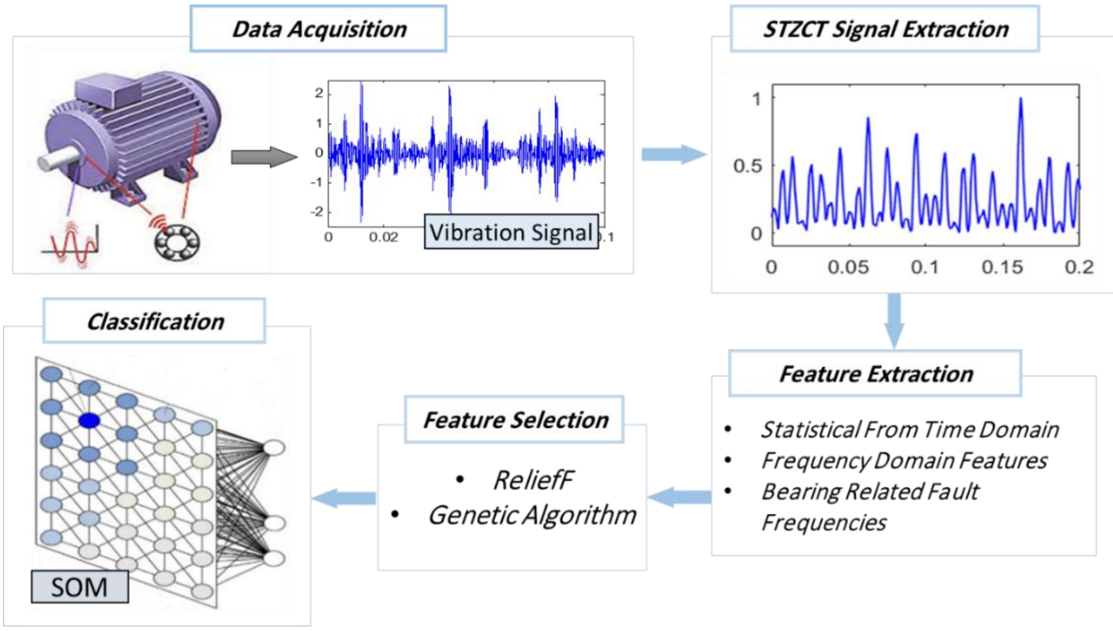

Fig. 1 Proposed Bearing Fault detection scheme

The zero-crossing rate of a given signal s(n) can be defined by the Equation (1).

$$ZCR = \sum_{n=-\infty}^{\infty} \left| \mathrm{sgn}(s(n) - \mathrm{sgn}(s(n-1)) \right| \quad (1)$$

Where $\mathrm{sgn}(\,)$ is the sign function defined in Equation (2).

$$\mathrm{sgn}(s(n)) = \begin{cases} 1 & if \;\; s(n) >= 0 \\ -1 & if \;\; s(n) < 0 \end{cases} \quad (2)$$

To perform short-time analysis, the vibration signal is segmented into shorter frames by applying a windowing function. Each segment undergoes ZCR calculation, allowing the technique to capture changes in the signal’s frequency content over time.

B. Features Extraction

After Performing the STZCT signal from the vibration signal, various statistical and frequency domain features are extracted from the STZCR to serve as fault indicators. These features provide critical insights into the signal characteristics, helping in the detection and diagnosis of bearing faults.

1) *Statistical Features:* these features are sensitive to impulse faults [13]. In this study, ten (10) statistical parameters (T1–T10) are extracted from the STZCT signal. The mathematical expressions for these parameters are provided in Table I.

2) *Frequency Domain Features:* Frequency domain analysis offers an alternative representation of a signal, uncovering information that might not be apparent in the time domain [2]. Ten (10) statistical features (F1–F10) are extracted from the frequency spectrum of the STZCR signal, as defined in Table I.

3) *Bearing Fault-Related Characteristic Frequencies:* These characteristic frequencies are crucial for diagnosing bearing faults. They include the **Rotating Speed Frequency (RSF)**, which corresponds to the bearing's rotating speed, the **Ball-Pass Frequency of the Outer Ring (BPFO)**, which occurs when balls pass over a defect on the outer ring, the **Ball-Pass Frequency of the Inner Ring (BPFI)**, associated with balls passing over a defect on the inner ring, and the **Ball-Spin Frequency (BSF)**,

ISSN: 1737-9288

which is the frequency at which the balls spin around their own axis. The mathematical expressions for these characteristic frequencies are presented in Table II.

TABLE I
TIME AND FREQUENCY DOMAIN FEATURES

Features from Time domain	Features from Frequency domain
$T_1=\frac{1}{n}\sum_{i=1}^{n}x_i$; $T_2=\left(\max(x_i)-\min(x_i)\right)/2$; $T_3=\sqrt{\frac{1}{N}\sum_{i=1}^{n}(x_i^2)}$; $T_4=\sqrt{\frac{1}{N}\sum_{i=1}^{N}(x_i-\bar{x})^2}$; $T_5=\frac{1}{N}\sum_{i=1}^{n}\left(\frac{x_i-\bar{x}}{\sigma}\right)^4$; $T_6=\frac{1}{N}\sum_{i=1}^{n}\left(\frac{x_i-\bar{x}}{\sigma}\right)^3$; $T_7=\max\lvert x_i\rvert\Big/\left(\frac{1}{N}\sum_{i=1}^{n}\sqrt{\lvert x_i\rvert}\right)^2$; $T_8=\max(\lvert x_i\rvert)\Big/\frac{1}{N}\sum_{i=1}^{n}\lvert x_i\rvert$ $T_9=\max\lvert x_i\rvert\Big/\sqrt{\frac{1}{N}\sum_{i=1}^{n}(x_i^2)}$; $T_{10}=\sqrt{\frac{1}{N}\sum_{i=1}^{n}(x_i^2)}\Big/\frac{1}{N}\sum_{i=1}^{n}\sqrt{\lvert x_i\rvert}$; where x_i is a vibration signal samples for i = 1,2,...,N, N is the number of data samples	$F_1=\sum_{k=1}^{K}\frac{s(k)}{K}$; $F_2=\sum_{k=1}^{K}\frac{(s(k)-F_1)^2}{(K-1)}$; $F_3=\sum_{k=1}^{K}\frac{(s(k)-F_1)^3}{(K(\sqrt{F_2})^3)}$; $F_4=\sum_{k=1}^{K}\frac{\sum_{k=1}^{K}(s(k)-F_1)^4}{KF_2^2}$ $F_5=\frac{\sum_{k=1}^{K}f_k s(k)}{\sum_{k=1}^{K}s(k)}$; $F_6=\sqrt{\frac{\sum_{k=1}^{K}(f_k-F_5)^2 s(k)}{K}}$ $F_7=\sqrt{\frac{\sum_{k=1}^{K}f_k^2 s(k)}{\sum_{k=1}^{K}s(k)}}$; $F_8=\sqrt{\frac{\sum_{k=1}^{K}f_k^4 s(k)}{\sum_{k=1}^{K}f_k^2 s(k)}}$; $F_9=\frac{\sum_{k=1}^{K}(f_k-F_5)^4 s(k)}{KF_6^4}$; $F_{10}=\frac{\sum_{k=1}^{K}(f_k-F_5)^{1/2}s(k)}{K\sqrt{F_6}}$ where $s(k)$ is a spectrum for k = 1,2,. . .,K, K is the number of spectrum lines; f_k is the frequency value of the k^{th} spectrum line

TABLE II
BEARING FAULT-RELATED FREQUENCIES COMPONENTS

Frequency component	BPFO	BPFI	BSF
Expression	$\frac{N}{2}\left[f_i\left(1-\frac{d\cos(\theta)}{D}\right)\right]$	$\frac{N}{2}\left[f_i\left(1+\frac{d\cos(\theta)}{D}\right)\right]$	$\frac{D}{2d}f_i\left[\left(1-\frac{d\cos(\theta)}{D}\right)^2\right]$

Where f_i is the shaft speed, d is the diameter of the rolling element, and D is the pitch diameter, θ is the contact angle

C. *Features Selection*

The goal of feature selection is to identify the most informative features for accurately diagnosing bearing faults, ensuring reliable classification [19]. In recent years, various feature selection techniques have been explored, such as Principal Component Analysis (PCA) [21], Sequential Backward Selection (SBS), ReliefF [22], and Genetic Algorithms (GA) [23]. Other popular methods include Minimum Redundancy Maximum Relevancy (mRMR) [24], Recursive Feature Elimination (RFE), and Mutual Information (MI), all of which help reduce data dimensionality while improving diagnostic performance by selecting the most relevant fault indicators.

1) *The ReliefF Technique:*

ReliefF is an efficient feature selection method used in problems with strong attribute dependencies [25]. Figure 2 outlines the algorithm.

ISSN: 1737-9288

```
Input : Gene variables and labels
Output : W for the gene rank
Set all weights W:=0;
Foreach Iteration n do
|   Randomly select an instance Insm;
|   Find K nearest hits H;
|   Foreach class c ≠ Labelm do
|   |   From class c find K nearest misses Mc;
|   End
|   Foreach gi do
|   |   Update Wi ;
|   End
End
```

Fig. 2 The reliefF algorithm.

It estimates the quality of attributes based on how well they distinguish between nearby instances. For a randomly selected instance (***Insm***) from class **L**, ReliefF identifies **K** nearest neighbors from the same class, called nearest hits (**H**), and **K** nearest neighbors from different classes, called nearest misses (**M**). The quality of each attribute is updated: if ***Insm*** and **H** have different values for an attribute, its quality decreases; if **Insm** and **M** have different values, its quality increases. This process is repeated n times as set by the user.

2) *Genetic Algorithm for Feature Selection:*

Genetic Algorithms (GAs) use evolutionary principles to select optimal features. Starting with a population of random chromosomes, representing different feature sets, the algorithm iterates through reproduction, crossover, and mutation to generate new solutions. Chromosomes are evaluated based on a fitness function, aiming to minimize within-class distance and maximize between-class distance. Each chromosome represents selected features (1 for inclusion, 0 for exclusion). The process continues until the best solution, representing the optimal feature subset, is found [22].

D. The Self Organizing Map (SOM)

The Self-Organizing Map (SOM) is an unsupervised neural network used for clustering and visualizing high-dimensional data [26]. It performs a nonlinear, topology-preserving mapping from high-dimensional input data onto a lower-dimensional space, typically forming a two-dimensional map of neurons [27].

A SOM consists of two layers: the input layer, with one neuron for each input variable, and the output layer, organized in a 2D grid for processing and mapping features (Fig. 3). Each neuron in the output layer is connected to all input neurons.

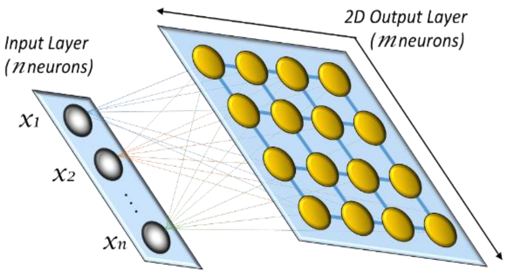

Fig. 3 SOM Architecture

During training, SOM adjusts its weight vectors to ensure that similar input data points activate neighboring neurons. For each training step, the algorithm identifies the best-matching unit (**bmu**) based on the smallest distance between the input vector and the weight vectors of all neurons:

$$\|X - W_{bmu}\| = \min i \left\{ \|X - W_i\| \right\} \quad , i \in \{1,...,m\} \tag{3}$$

where W_{bmu} is the best-matching unit weight vector.

Once the bmu is identified, the weights of the bmu and its neighbors are updated using the rule:

$$W_i(\tau+1) = W_i(\tau) + \varepsilon(\tau) h_{bmu}(i,\tau)\left[X(\tau) - W_i(\tau)\right] \tag{4}$$

ISSN: 1737-9288

Where τ is time, $\varepsilon(\tau)$ is a learning rate and $h_{bmu}(i, \tau)$ is defined as the neighborhood kernel function around the *bmu*. Usually, $\varepsilon(\tau)$ is a decreasing function of time and should be between 0 and 1. In this paper the Gaussian neighborhood function is chosen.

III. EXPERIMENTAL SETUP

The proposed fault detection method is applied to bearing fault vibration signal data obtained from the Case Western Reserve University Bearing Data Center [28]. In this setup, vibration signals are captured at a sampling rate of 12 kHz using accelerometers mounted on the motor housing at the drive end of a three-phase induction motor. The motor is coupled to a dynamometer, which serves as the load, as illustrated in Figure 4.

In this work, we investigate four distinct operating conditions: normal operation (NO), outer race fault (ORF), inner race fault (IRF), and ball fault (BF), with a fault diameter of 0.021 inches. Each experiment is repeated under four different load conditions: 0, 1, 2, and 3 Hp.

The experimental data is segmented into 448 samples (112 samples per operating condition), each containing 4096 data points. The Short-Time Zero Crossing Rate (STZCR) is then computed, and features are extracted using a frame size of 40 samples and a frame shift of 10 samples. A total of 24 features are calculated for each segment, resulting in a dataset with dimensions of 448 × 24. Two-thirds of the dataset is used to train the Self-Organizing Map (SOM), with the remaining portion reserved for testing. A four-class classification process is employed to evaluate the system's performance, corresponding to the four operating conditions. Since SOM is an unsupervised neural network, labels are assigned to each case as detailed in Table III.

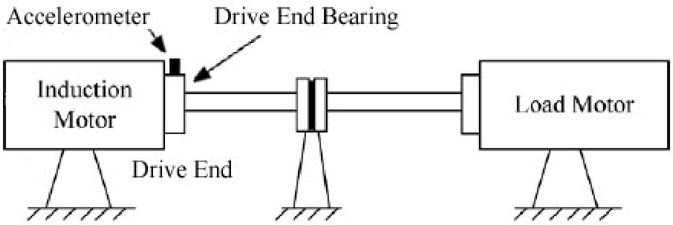

Fig. 4 The experimental test rig scheme

TABLE IIII
DESCRIPTION OF CLASSIFICATION TASKS

Bearing Condition	Associated Labels
Normal	NOR
Ball Fault	BLF
Inner Race Fault	IRF
Outer Race Fault	ORF

IV. RESULTS AND DISCUSSION

Following the calculation of features and the construction of the dataset, three sets of extracted features were evaluated individually to assess their performance in fault classification.

The histogram in Fig. 5 illustrates that the time-domain features derived from the Short-Time Zero Crossing Rate (STZCR) achieved a classification accuracy of 90.97%. In contrast, the bearing fault-related characteristic frequencies yielded a lower accuracy of 87.5%. Notably, the frequency-domain features of the STZCR produced the highest classification accuracy at 96.52%. So it can be concluded that the frequency domain of the STZCR of the vibration signal carry a lot of information about the bearing condition.

ISSN: 1737-9288

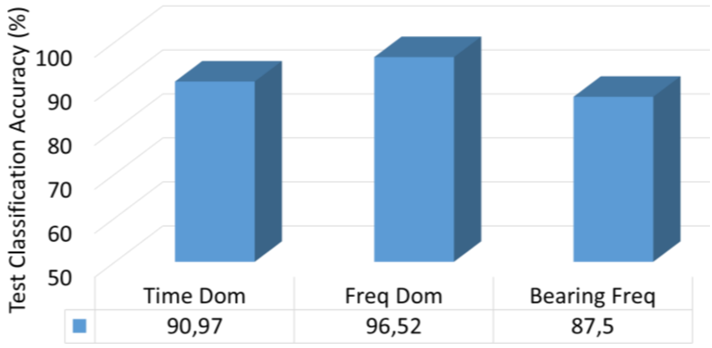

Fig. 5 Performance comparison of features from the three features extraction methods

These results underscore the efficacy of the frequency-domain features derived from the STZCR of the vibration signal in capturing relevant information regarding bearing conditions. The superior performance of frequency-domain features suggests that they provide deeper insights into the frequency components associated with various fault types.

After evaluating the feature extraction techniques individually, we applied dimensionality reduction to the entire dataset using the ReliefF and Genetic Algorithm (GA) feature selection approaches. Both techniques were implemented to determine the optimal number of selected features, ranging from one to twenty-four (total number of features).

Figure 6 illustrates the classification performance of the trained Self-Organizing Map (SOM) in relation to the number of features selected by these two algorithms. The analysis reveals that the optimal number of features selected is eight (8) for the ReliefF technique and seventeen (17) for the GA technique. Notably, both of these feature selections resulted in improved classification accuracy compared to the original feature extraction techniques. Specifically, the ReliefF method achieved the highest accuracy of 99.30%, surpassing the GA technique's accuracy of 97.92%.

Following the training phase and evaluation of classification performance, the results of the Kohonen map (SOM) can also be interpreted through a two-dimensional topological network, which includes the associated labels for each class. This representation provides a valuable topological understanding of the training data distribution on the map and offers clear visualization of the inter-class distances. The proximity of the mapped classes indicates the relationship and similarities between different fault conditions, thereby enhancing the interpretability of the SOM model and supporting effective fault diagnosis.

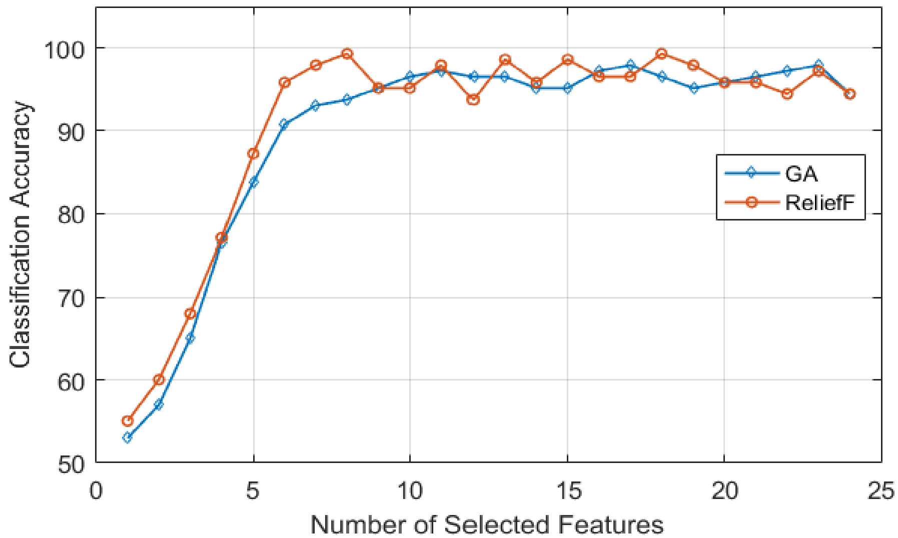

Fig. 6 Classification accuracy vs Number of selected features using ReliefF and GA techniques

Figure 7 illustrates the trained Self-Organizing Map (SOM) using the features selected by the ReliefF and Genetic Algorithm (GA) approaches. Both SOM maps exhibit a distinct separation among the four bearing condition classes. The samples are clearly organized on the map into four well-defined clusters, with significant distances between them. This spatial

ISSN: 1737-9288

arrangement indicates the effectiveness of the selected features in capturing the underlying patterns in the data, thereby facilitating accurate classification of the different bearing conditions.

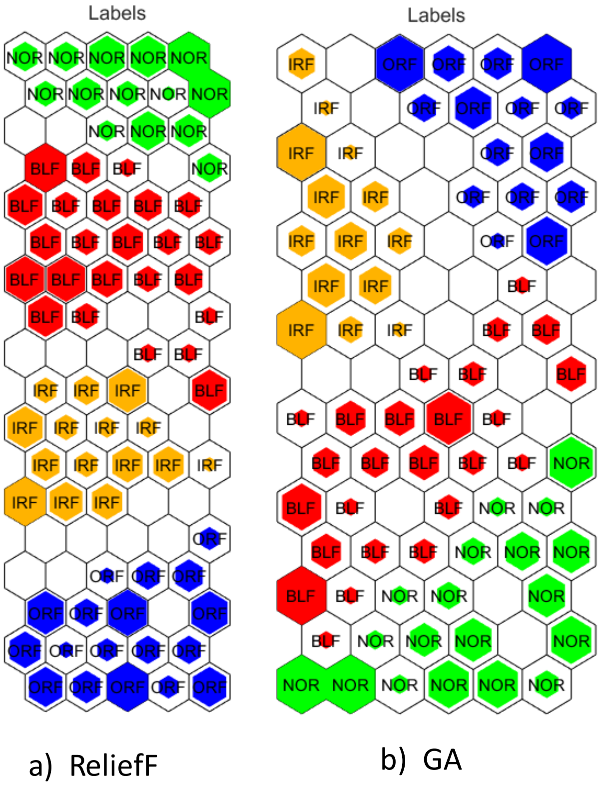

Fig. 7 The obtained trained Maps.

V. Conclusions

This study introduces a novel methodology for detecting bearing faults in electric motors, leveraging the Short Time Zero Crossing Rate (STZCR) of vibration signals in conjunction with Self-Organizing Maps (SOM) and feature selection techniques. By integrating multiple signature analysis methods from the time domain, frequency domain, and bearing fault-related frequencies, our approach enhances fault detection and classification under variable load conditions. The experimental results demonstrate that the combination of STZCR and SOM, particularly when enhanced by feature selection, significantly improves the quality of the learned map and reduces training time.

Future work will focus on implementing this automatic bearing fault detection system in real-time applications and exploring its capabilities for fault severity evaluation.

References

[1] IAS Motor Reliability Working Group, “Report of large motor reliability survey of industrial and commercial installations: Part I and Part II,” IEEE Trans. Ind. Appl., vol. 21, no. 4, pp. 853–872, 1985.

[2] A. Das and S. Ray, “A review on diagnostic techniques of bearing fault and its modeling in induction motor,” in 2020 IEEE Calcutta Conf. (CALCON), Kolkata, India, 2020, pp. 502–505, doi: 10.1109/CALCON49167.2020.9106511.

[3] P. Gupta and M.K. Pradhan, “Fault detection analysis in rolling element bearing: A review,” Mater. Today: Proc., vol. 4, no. 2, part A, pp. 2085–2094, 2017, doi: 10.1016/j.matpr.2017.02.054.

[4] I. El-Thalji and E. Jantunen, “A summary of fault modeling and predictive health monitoring of rolling element bearings,” Mech. Syst. Signal Process., vol. 60, pp. 252–272, 2015.

[5] M. Altaf, T. Akram, M.A. Khan, M. Iqbal, M.M.I. Ch, and C.-H. Hsu, “A new statistical features-based approach for bearing fault diagnosis using vibration signals,” Sensors, vol. 22, no. 5, p. 2012, 2022, doi: 10.3390/s22052012.

[6] J. Zhou, Y. Qin, L. Kou, M. Yuwono, and S. Su, “Fault detection of rolling bearing based on FFT and classification,” J. Adv. Mech. Des. Syst. Manuf., vol. 9, no. 5, 2015, doi: 10.1299/jamdsm.2015jamdsm0056.

ISSN: 1737-9288

[7] H. Gao, L. Liang, X. Chen, and G. Xu, “Feature extraction and recognition for rolling element bearing fault utilizing short-time Fourier transform and non-negative matrix factorization,” Chin. J. Mech. Eng., vol. 28, no. 1, pp. 96–105, 2015.
[8] J. Cai and Y. Xiao, “Time-frequency analysis method of bearing fault diagnosis based on the generalized S transformation,” J. Vibroeng., vol. 19, no. 6, pp. 4221–4230, Sep. 2017, doi: 10.21595/jve.2017.18244.
[9] J.B. Ali, N. Fnaiech, L. Saidi, B. Chebel-Morello, and F. Fnaiech, “Application of empirical mode decomposition and artificial neural network for automatic bearing fault diagnosis based on vibration signals,” Appl. Acoust., vol. 89, pp. 16–27, 2015.
[10] R. Yan, R.X. Gao, and X. Chen, “Wavelets for fault diagnosis of rotary machines: A review with applications,” Signal Process., vol. 96, pp. 1–15, 2014.
[11] M. Alonso-González, V.G. Díaz, B.L. Pérez, B.C.P. G-Bustelo, and J.P. Anzola, “Bearing fault diagnosis with envelope analysis and machine learning approaches using CWRU dataset,” IEEE Access, vol. 11, pp. 57796–57805, 2023, doi: 10.1109/ACCESS.2023.3283466.
[12] P.E. William and M.W. Hoffman, “Identification of bearing faults using time domain zero-crossings,” Mech. Syst. Signal Process., vol. 25, no. 8, pp. 3078–3088, 2011, doi: 10.1016/j.ymssp.2011.06.001.
[13] S. Haroun, A.N. Seghir, and S. Touati, “Feature selection for enhancement of bearing fault detection and diagnosis based on self-organizing map,” in Recent Advances in Electrical Engineering and Control Applications, Springer, 2017, pp. 233–246.
[14] P. Santos, L.F. Villa, A. Reñones, A. Bustillo, and J. Maudes, “An SVM-based solution for fault detection in wind turbines,” Sensors, vol. 15, no. 3, pp. 5627–5648, 2015.
[15] A.S. Raj and N. Murali, “Early classification of bearing faults using morphological operators and fuzzy inference,” IEEE Trans. Ind. Electron., vol. 60, no. 2, pp. 567–574, 2013.
[16] I.Y. Onel, K.B. Dalci, and I. Senol, “Detection of bearing defects in three-phase induction motors using Park’s transform and radial basis function neural networks,” Sadhana, vol. 31, no. 3, pp. 235–244, 2006.
[17] A. Choudhary, T. Mian, and S. Fatima, “Convolutional neural network based bearing fault diagnosis of rotating machine using thermal images,” Measurement, vol. 176, 2021, 109196, doi: 10.1016/j.measurement.2021.109196.
[18] J. Bei, C. Lu, X. Tao, and Z. Wang, “Performance assessment for rolling bearing based on EMD and SOM,” in FITMSE 2012, Lect. Notes Inf. Technol., vol. 14, pp. 95–99, 2012.
[19] S. Haroun, A.N. Seghir, and S. Touati, “Stator inter-turn fault and voltage unbalance detection and discrimination approach for a reactor coolant pump,” in Proc. 3rd Int. Conf. Systems and Control ICSC, pp. 99–104, 2013.
[20] A.H. Omar, “Audio segmentation and classification,” PhD thesis, Kgs. Lyngby, 2005.
[21] J. Shen and F. Xu, “Method of fault feature selection and fusion based on poll mode and optimized weighted KPCA for bearings,” Measurement, vol. 194, 2022, 110950, doi: 10.1016/j.measurement.2022.110950.
[22] B. Li, P. Zhang, G. Ren, and Z. Xing, “A two stage feature selection method for gear fault diagnosis using ReliefF and GA-wrapper,” in Proc. Int. Conf. Measuring Technology Mechatronics Autom., 2009, pp. 578–581.
[23] N.T. Nguyen, H.H. Lee, and J.M. Kwon, “Optimal feature selection using genetic algorithm for mechanical fault detection of induction motor,” J. Mech. Sci. Technol., vol. 22, no. 3, pp. 490–496, 2008.
[24] S. Haroun, A.N. Seghir, and S. Touati, “Multiple features extraction and selection for detection and classification of stator winding faults,” IET Elect. Power Appl., vol. 12, no. 4, pp. 339–346, 2018, doi: 10.1049/iet-epa.2017.0457.
[25] M. Robnik-Sikonja and I. Kononenko, “Theoretical and empirical analysis of ReliefF and RReliefF,” Mach. Learn., vol. 53, pp. 23–69, 2003.
[26] T. Kohonen, Self-Organizing Maps, 3rd ed. Berlin: Springer, 2001.
[27] J.M. Bossio and C.H. De Angelo, “Self-organizing map approach for classification of mechanical and rotor faults on induction motors,” Neural Comput. Appl., vol. 23, pp. 41–51, 2013.
[28] Case Western Reserve University, “Bearing data centre,” [Online]. Available: http://www.eecs.cwru.edu/laborator/bearing. [Accessed: Jun. 20, 2024].

ISSN: 1737-9288